

**Jahn-Teller effect in the emission and absorption spectra of ZnS:Cr<sup>2+</sup> and ZnSe:Cr<sup>2+</sup>**

G. Bevilacqua

*INFN and Dipartimento di Fisica, Via Roma 56, 53100 Siena, Italy*

L. Martinelli

*INFN and Dipartimento di Fisica "E. Fermi," Via Buonarroti, 2, 56100 Pisa, Italy*

E. E. Vogel and O. Mualin

*Departamento de Física, Universidad de La Frontera, Casilla 54-D, Temuco, Chile*

(Received 4 November 2003; published 26 August 2004)

The Jahn-Teller effect is invoked to explain the fine structure (isolated zero-phonon lines) observed in both the infrared emission and absorption spectra of substitutional Cr<sup>2+</sup> impurities in ZnSe and ZnS. The ground <sup>5</sup>D<sub>2</sub> term of Cr<sup>2+</sup> is split by crystal field into a <sup>5</sup>T<sub>2</sub> ground multiplet and an excited <sup>5</sup>E multiplet. We look at transitions among levels belonging to these two multiplets, which happen to be in the near infrared region. Spin-orbit and spin-spin interactions are taken into account. The Jahn-Teller coupling is introduced as a linear coupling considering both  $\epsilon$  and  $\tau_2$  phonons. The Lanczos-recursion procedure with a proper choice of the initial state is used to calculate the vibronic functions and energies. It is found that  $\epsilon$  modes only lead to intensities that do not agree well with those of the zero-phonon doublet observed both in emission and absorption in the cases of ZnS and ZnSe, while  $\tau_2$  modes give a good explanation of transition energies and transitions strengths in the same cases. A discussion of the relatively high strength of the vibronic coupling for Cr in comparison with other impurities in the same compounds is also included.

DOI: 10.1103/PhysRevB.70.075206

PACS number(s): 71.70.Ej, 71.55.Gs

**I. INTRODUCTION**

The infrared properties of chromium impurities in ZnS and ZnSe (as well as other compounds) have been known for three decades since the pioneering work by Vallin *et al.*,<sup>1</sup> followed by experimental works of similar resolution and theoretical work based on such data.<sup>2-7</sup> The importance of the Jahn-Teller (JT) effect in the specific heat and magnetic properties of these systems was recognized and some possible coupling mechanisms and competing distortions have been subsequently postulated.<sup>8</sup> More recently, higher resolution luminescence spectra and well-resolved absorption experiments added information to the infrared properties of Cr<sup>2+</sup> in these compounds, thus motivating the calculations in the present paper.<sup>9-11</sup> In the experimental work a Jahn-Teller energy  $E_{JT}=370\text{ cm}^{-1}$  was ventured for the case of ZnSe based on general arguments indicating the presence of a moderate or strong JT coupling. However, up to now no precise analysis is known accounting for both energies and relative line strengths for the zero-phonon doublet appearing both in the emission and absorption spectra of ZnS:Cr<sup>2+</sup> and ZnSe:Cr<sup>2+</sup>. This is precisely the main aim of the present paper, where we will use well-established techniques to calculate energy levels and wave functions for both systems. The explanation of the spectra will allow us to obtain more precise values for the coupling constants. This will be compared to values of the parameters for the similar ions (V, Fe) in the same compounds thus pointing out to a more general analysis. Additionally, we will bear in mind the behavior of the same substitutional ion in GaAs,<sup>12</sup> having the same crystalline structure, for a general comparison.

Interest in this subject has been revitalized since the variety of magnetic properties shown by these systems in the

heavy doped samples. Thus both ZnS:Cr<sup>2+</sup> and ZnSe:Cr<sup>2+</sup> are diluted ferromagnetic semiconductors with potential use as spintronic devices.<sup>13</sup>

The article is organized as it follows. In the next section, general crystal-field theory is presented combined with the presentation of experimental spectra showing the need for extra interactions to explain the doublet of bands in both absorption and emission spectra for both systems. In Sec. III, the JT coupling is introduced, results are obtained and a general analysis is done as to single out the most relevant modes responsible for the coupling in each system. Then, energy levels and wave functions are evaluated leading to transition lines and relative intensities that agree well with both absorption and emission spectra in both systems. Finally, in Sec. IV some concluding remarks are formulated.

**II. CRYSTAL FIELD AND REVIEW OF EXPERIMENTS**

ZnS is found mostly as a cubic crystal with the zincblende structure, which is the usual crystal phase for ZnSe also. Cr appears as a substitutional impurity at the cation site, surrounded by four anions (S or Se) in tetrahedral coordination. We assume here a non-distorted surrounding as a starting point, which means the presence of point-group  $T_d$  at the Cr site. This impurity presents itself as a doubly ionized atom, Cr<sup>2+</sup>, after closing all bonds. Using the free-ion model, the ground configuration is <sup>5</sup>D according to Hund's rules. Crystalline field further splits this configuration as well as excited multiplets causing small admixtures among the otherwise pure atomic levels. As a result of this process the <sup>5</sup>D term splits into a ground multiplet of symmetry  $T_2$  and an excited multiplet  $E$ , with degeneracies 15 and 10, respec-

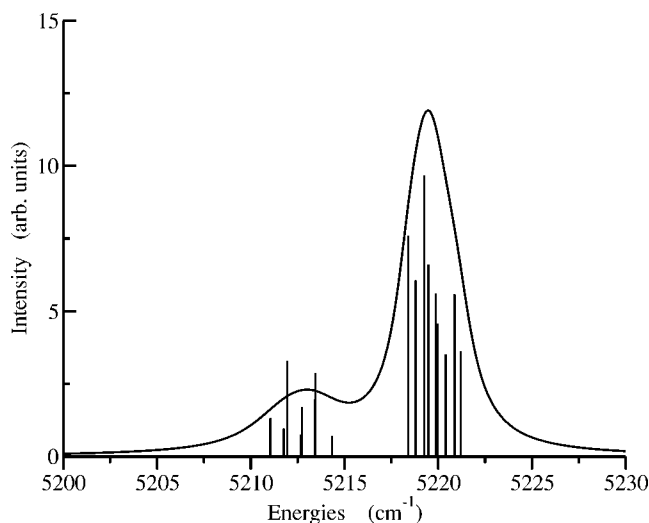


FIG. 1. Emitted lines as predicted by coupling to  $\epsilon$  modes only. Half-widths for the Lorentzian line shapes are  $1 \text{ cm}^{-1}$  for lines around  $5218 \text{ cm}^{-1}$  (with large component of zero-phonon vibronic levels) and  $2 \text{ cm}^{-1}$  for the other lines with large components of one-phonon lines. This spectrum reproduces well the energy positions but not the intensities (compare to Fig. 1 of Ref. 9).

tively. Spin-orbit and spin-spin interactions further split and rearrange these levels producing irregular “ladders” of energy levels. This is a well-known energy level diagram and can be viewed in the literature<sup>14</sup> (see Fig. 1 in this reference). Then electric-dipole transitions can lead to emissions or absorptions among levels of these two multiplets.

Neither absorption or emission spectra measured in ZnS or ZnSe match this simple description. Let us review next the main characteristics of the two spectra (emission and absorption) for each of the systems (ZnS:Cr<sup>2+</sup> and ZnSe:Cr<sup>2+</sup>).

In ZnS:Cr<sup>2+</sup> the near infrared emission spectrum<sup>9-11</sup> presents a clear threshold line at  $5218 \text{ cm}^{-1}$ , then a stronger zero-phonon line at  $5212 \text{ cm}^{-1}$ , followed by some weak structures before the emission curve raises continuously due to phonon-assisted transitions (in the range that goes from  $5160$  to  $5190 \text{ cm}^{-1}$  zero-phonon lines due to off-cubic sites are present but they are not covered in the present analysis). On the other hand, the near infrared absorption spectrum presents a strong line at  $5218 \text{ cm}^{-1}$ , followed by a weaker band at  $5212 \text{ cm}^{-1}$  and some very weak structure at lower energy. Three features are of importance for the present work: a) The correspondence between emission and absorption spectra is total with respect to the central energy of the bands; b) the energy difference between the center of these two bands is  $6 \text{ cm}^{-1}$ ; c) the width of both lines is  $4$  to  $5 \text{ cm}^{-1}$ , much larger than spectral resolution which is an indication of a composed band.

In the case of ZnSe:Cr<sup>2+</sup> the near infrared luminescence spectrum<sup>10,11</sup> exhibits also a main doublet, with the threshold line at  $4971 \text{ cm}^{-1}$ , followed by a stronger line at  $4964 \text{ cm}^{-1}$ . The weaker structures (if any) are overlapped by phonon assisted transitions that begin right on the low-energy end of the second peak. The corresponding absorption spectrum replicates a pair of lines at the same energies, but the line at  $4964 \text{ cm}^{-1}$  is much weaker than the threshold absorption at

$4971 \text{ cm}^{-1}$ . Similar to the previous case, these two transitions look wider than experimental resolution; the separation between the centers of these two bands is  $7 \text{ cm}^{-1}$ .

The argument given above in the sense that each band of the doublet is composed of several lines is also supported by the explanation given<sup>12</sup> to the absorption spectrum of GaAs:Cr<sup>2+</sup>. Due to the general structural and electronic similarities between that system and ours the general aspect of the spectra cannot be entirely different.

The close doublet of lines, both in emission and absorption, cannot be explained by simple crystal field theory. A JT effect is now introduced to explain the spectra in both ZnS:Cr<sup>2+</sup> and ZnSe:Cr<sup>2+</sup>.

### III. MODEL HAMILTONIAN, RESULTS AND ANALYSIS

In general terms the total Hamiltonian of this system can be written in the form:

$$H = H_e + H_{so} + H_{ss} + H_L + H_{e-L}. \quad (1)$$

where the sum  $H_e + H_{so} + H_{ss}$  represents the electronic Hamiltonian including crystalline field, followed by the spin-orbit interaction  $\lambda \mathbf{S} \cdot \mathbf{L}$ , and spin-spin interaction  $-\rho[(\mathbf{L} \cdot \mathbf{S})^2 + 1/2(\mathbf{L} \cdot \mathbf{S})]$  whose explicit form can be obtained with standard methods.  $H_L$  is the vibrational Hamiltonian associated with the lattice, which is taken here in the harmonic approximation.  $H_{e-L}$  is the electron-lattice interaction, namely, this term represents the vibronic or JT coupling including electronic coordinates as well as vibrational normal modes. In the following  $H_L$  and  $H_{e-L}$  should be considered multiplied by the unity operator in the spin space.

Crystal field parameter  $10|Dq|$  is taken as to yield the threshold line in each case ( $5218 \text{ cm}^{-1}$  for ZnS and  $4971 \text{ cm}^{-1}$  for ZnSe). Atomic parameters for chromium are taken directly from the literature<sup>1,15</sup> as previously reported. Namely  $\lambda = 57 \text{ cm}^{-1}$  and  $\rho = 0.39 \text{ cm}^{-1}$ . Small deviations from these values have been used too but this is not the main issue here.

The most important phonons in terms of the coupling are those that produce displacements of the surrounding ions toward the central Cr impurity breaking the local symmetry. This allows us to use the cluster approximation<sup>18</sup> where only the four anions sitting at the vertices of a regular tetrahedron are considered. We neglect, as usual, the total symmetric mode (breathing mode), then there are five nontrivial possible coupling modes: the two normal modes behaving as basis functions for the  $\epsilon$  representation of the  $T_d$  point group and the three normal modes transforming as basis functions for the  $\tau_2$  irreducible representation. Let us designate by  $q_\theta$ ,  $q_\epsilon$ ,  $\omega_\epsilon$  and  $q_x$ ,  $q_y$ ,  $q_z$ ,  $\omega_\tau$  the normal modes coordinates and frequency of  $\epsilon$  and  $\tau_2$ , respectively. Using usual second quantized notation we can write for the ground multiplet:

$$H_{L\epsilon} = \hbar \omega_\epsilon (a_\theta^\dagger a_\theta + a_\epsilon^\dagger a_\epsilon + 1), \quad (2)$$

$$H_{L\tau_2} = \hbar \omega_\tau (a_x^\dagger a_x + a_y^\dagger a_y + a_z^\dagger a_z + \frac{3}{2}), \quad (3)$$

$$H_L = H_{L\epsilon} + H_{L\tau_2}. \quad (4)$$

The components of the coupling term can be written as

$$H_{e-L\epsilon} = \sqrt{\hbar\omega_\epsilon E_{JT}^{(\epsilon)}} \sum_{\alpha} (a_{\alpha}^{\dagger} + a_{\alpha}) D_{\alpha}, \quad (5)$$

$$H_{e-L\tau} = \sqrt{\hbar\omega_\tau E_{JT}^{(\tau)}} \sum_i (a_i^{\dagger} + a_i) D_i, \quad (6)$$

$$H_{e-L} = H_{e-L\epsilon} + H_{e-L\tau_2}, \quad (7)$$

with  $\alpha = \theta, \epsilon$  and  $i = x, y, z$ . Here  $E_{JT}^{(\epsilon)}$  and  $E_{JT}^{(\tau)}$  are the JT energies for modes  $\epsilon$  and  $\tau_2$ , respectively. Electronic operators  $D_{\alpha}$  and  $D_i$  have the form:<sup>16</sup>

$$D_{\theta} = \begin{pmatrix} -\frac{1}{2} & 0 & 0 \\ 0 & -\frac{1}{2} & 0 \\ 0 & 0 & 1 \end{pmatrix}, \quad D_{\epsilon} = \begin{pmatrix} \frac{\sqrt{3}}{2} & 0 & 0 \\ 0 & -\frac{\sqrt{3}}{2} & 0 \\ 0 & 0 & 0 \end{pmatrix},$$

$$D_x = \begin{pmatrix} 0 & 0 & 0 \\ 0 & 0 & -1 \\ 0 & -1 & 0 \end{pmatrix}, \quad D_y = \begin{pmatrix} 0 & 0 & -1 \\ 0 & 0 & 0 \\ -1 & 0 & 0 \end{pmatrix},$$

$$D_z = \begin{pmatrix} 0 & -1 & 0 \\ -1 & 0 & 0 \\ 0 & 0 & 0 \end{pmatrix}.$$

The Huang-Rhys factor  $S$  is generally defined as  $S = E_{JT}/\hbar\omega$ . In the present problem it is possible to define  $S_{\epsilon}$  and  $S_{\tau}$  according to each coupling.

In the upper multiplet a similar coupling can be introduced, but only with  $\epsilon$  distortions, as it is well known,<sup>16</sup> and the appropriate coupling matrices are:

$$D_{\theta} = \begin{pmatrix} 1 & 0 \\ 0 & -1 \end{pmatrix}, \quad D_{\epsilon} = \begin{pmatrix} 0 & 1 \\ 1 & 0 \end{pmatrix},$$

Once the coupling modes are decided, calculation of energy levels and wave functions can be done by means of the Lanczos-recursion method,<sup>19,20</sup> with a proper number of over-recursions. We refer the reader to the literature for details of the application of this method and calculation procedures.<sup>21,22</sup>

Results and their analysis will be done separately for each compound beginning with ZnS, where there is well-resolved experimental information<sup>9-11</sup> and phonon assisted transitions are far from the main doublet.

### A. Results and discussion for ZnS:Cr<sup>2+</sup>

First, the JT coupling for the upper <sup>5</sup>E multiplet is considered with  $\epsilon$  phonons as required by symmetry. The fact that only two broad bands are seen in emission is an indication that all low-energy vibronic levels of the upper multiplet are compressed in a range of no more than 3 cm<sup>-1</sup>, in a way similar to what was found for the similar ion V<sup>2+</sup> in these same systems.<sup>17</sup> Coupling phonon is taken at energy equal to

that used in the coupling for the lower multiplet, that is at  $\hbar\omega' = \hbar\omega_{\epsilon, \tau}$  and the JT energy  $E_{JT}'$  is varied in a broad range. Here and in the rest of the paper primes are used for parameters referring to the coupling to the upper E multiplet. It turns out that the actual spectrum is little sensitive to the value of  $E_{JT}'$  for the upper multiplet, then there is a wide range of possible values for this parameter yielding all upper levels within 3 cm<sup>-1</sup> as desired. In summary, for any coupling model in <sup>5</sup>T multiplet we have taken fixed the crystal-field parameter to produce the main transition at 5218 cm<sup>-1</sup>, then  $E_{JT}'$  is taken in such a way to produce the spread of 3 cm<sup>-1</sup> in the upper multiplet; the JT energy in the lower multiplet is varied freely for each possible coupling mode.

In a first attempt we consider the JT coupling to the <sup>5</sup>T multiplet as due to  $\epsilon$  modes only. It was possible to find a parameter zone where the energy of the vibronic levels gave a good explanation of observed lines for ZnS:Cr<sup>2+</sup>, both in emission and absorption. However, it was never possible to reach an agreement in the intensities of the lines even after a thorough variation of parameters.

Figure 1 gives an idea of what the main emission lines would be when only coupling to  $\epsilon$  modes is considered. Since the representation technique used in this figure is later used in some other figures below, let us explain its meaning. The energy of the spectral absorption or emission is represented by a line at the energy according to the scale given in the abscissa. The relative intensity of that transition is given by the height of the line. The curve over the lines corresponds to a superposition of intensities using Lorentzian line shapes with arbitrary but reasonable half-widths as indicated in the corresponding figure caption. In general, width was linearly increased for lines involving higher levels as they progressively involve components with more phonon overtones thus widening the vibronic level. If the emission spectrum predicted by Fig. 1 is compared to the corresponding one in the experimental paper,<sup>9-11</sup> it is observed that positions of the energy lines agree with experiment but relative intensities are in great disagreement. Actually, the experiment gives the opposite, namely, the peak at 5212 cm<sup>-1</sup> much higher and wider than the peak at 5218 cm<sup>-1</sup>.

Figure 1 was obtained after using  $\hbar\omega_{\epsilon} = 100$  cm<sup>-1</sup> for reasons to become clear below. However, there is no noticeable improvement in the intensity of the lines as compared to experiments upon varying the value of  $\hbar\omega_{\epsilon}$  around 100 cm<sup>-1</sup>. Then  $\tau_2$  modes are recovered and treated as the only responsible modes, just as we did with the  $\epsilon$  modes.

Then we now go back to the original Hamiltonian switching off  $\epsilon$  modes while switching on  $\tau_2$  modes. We will do a complete exercise to show that the energy of the coupling mode comes out readily from the parameter variation. In Fig. 2 we present a composition of calculated emission curves (using the same technique as presented in Fig. 1) for three values of  $\hbar\omega_{\tau}$ , namely 90, 100, and 120 cm<sup>-1</sup>, from bottom to top. It follows that it is only for the second of these curves that the main features of the experiments are well represented. As it can be seen a first band at 5218 cm<sup>-1</sup> is produced, followed by a higher and wider band centered at 5212 as shown by the experiments. Some extra activity is noticed

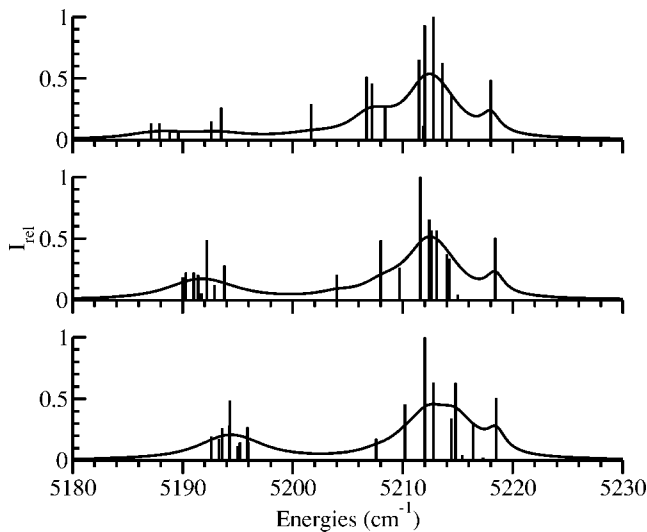


FIG. 2. Emitted lines predicted by coupling the  ${}^5T_2$  multiplet to  $\tau_2$  modes only. Half-widths are  $1\text{ cm}^{-1}$  for lines around  $5218\text{ cm}^{-1}$ ,  $2\text{ cm}^{-1}$  for lines around  $5212\text{ cm}^{-1}$  and  $3\text{ cm}^{-1}$  for the other lines. Energy of the coupling mode is  $90\text{ cm}^{-1}$  at the bottom,  $100\text{ cm}^{-1}$  at the center and  $120\text{ cm}^{-1}$  at the top.

toward lower energies as also shown by the experimental spectra.

The way curves in Fig. 2 (and others in this paper) are constructed is the same as indicated before at the beginning of this subsection. It has been chosen  $\hbar\omega' = \hbar\omega_\tau$  and a proper value for  $E'_{JT}$  results to be  $370\text{ cm}^{-1}$ . When  $E_{JT}^{(\tau)}$  (lower multiplet) is varied freely it is found that energies of vibronic levels corresponding to the lower multiplet are quite sensitive to the value of  $E_{JT}^{(\tau)}$  as illustrated in Fig. 3 for the case  $\hbar\omega_\tau = 100\text{ cm}^{-1}$ . It is here that a zone is found where the energy difference between lower vibronic levels and upper vibronic levels yields approximately  $6\text{ cm}^{-1}$  for the case of  $\text{ZnS:Cr}^{2+}$ .

As can be seen from Fig. 3, such value is approximately  $E_{JT}^\tau = 260\text{ cm}^{-1}$  for the case  $\hbar\omega_\tau = 100\text{ cm}^{-1}$ , which also leads

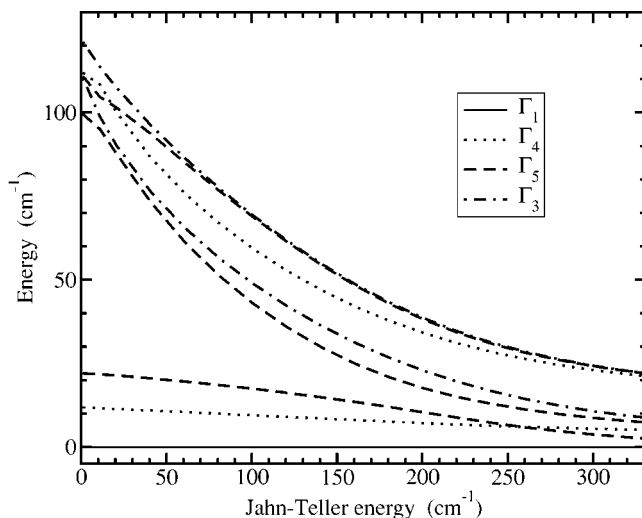


FIG. 3. Energy of vibronic levels as functions of  $E_{JT}^{(\tau)}$  for a coupling phonon of energy  $\hbar\omega_\tau = 100\text{ cm}^{-1}$ .

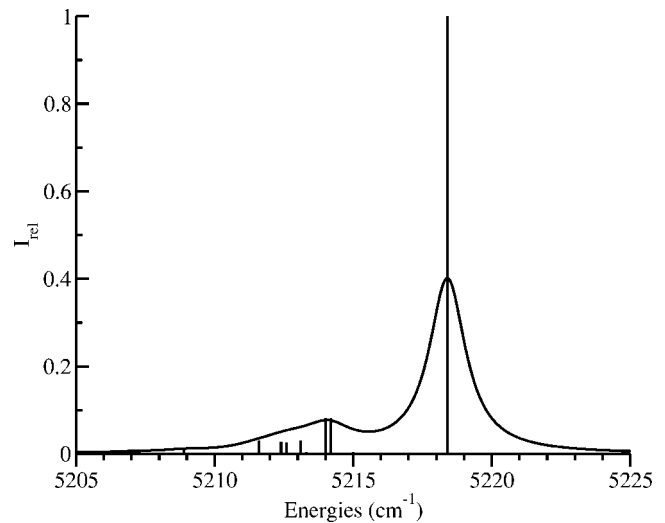


FIG. 4. Absorption spectrum for  $\text{ZnS:Cr}^{2+}$  directly calculated using the same wave functions used to calculate emission spectrum in the central part of Fig. 2.

to appropriate relative intensity of the lines. Eventually, approximate explanation of the spectra can also be possible at increasing values of  $E_{JT}^\tau$ , but this would also mean increasing activity around  $5200\text{ cm}^{-1}$ , where nothing is observed in the emission spectra.<sup>9-11</sup> The broad structure seen in the luminescence spectrum of  $\text{ZnS:Cr}$  at lower energies (more strongly observed for the case of  $\text{ZnSe}$ ) is the result of emissions involving higher-order phonon vibronic levels or phonon assisted transitions. Our model, although limited as phonon occupation number increases, predicts many medium to low intensity lines for energies less than  $5100\text{ cm}^{-1}$  (not shown). We do not attempt an adjustment here, not only due to the limitations of the method, but also because the shape of these broad bands is very sensitive to the amount of doping (see Fig. 3 of Ref. 9) and excitation source in the experiments (see Fig. 6.12 of Ref. 11).

With the main vibronic levels reached in this way and without any further adjustment, the fine structure of the absorption spectrum is now directly calculated, introducing the appropriate Boltzmann population factors corresponding to liquid helium temperature. The calculated spectrum corresponding to  $\text{ZnS:Cr}^{2+}$  is presented in Fig. 4, resembling quite well the measured spectrum.<sup>9-11</sup>

The reason to use  $\hbar\omega_\epsilon = 100\text{ cm}^{-1}$  in Fig. 1 is precisely to allow a comparison between that figure and the central curve in Fig. 2. As can be seen, the predicted relative intensities of the peaks for the luminescence spectrum is better described by means of coupling to  $\tau_2$  modes. These arguments do not rule out a weak coupling to modes  $\epsilon$ , which give good explanation of the energy difference as already stated above. However, the relative line intensity suggests that the dominant coupling is to  $\tau_2$  modes, which is assumed here as the only coupling mode from now on.

In summary, for plausible phonon energies vibronic levels are found varying  $E_{JT}^{(\tau)}$ . For the particular value at which the appropriate energy difference is found, oscillator strengths involving vibronic levels are calculated. Fine structures of emission and absorption spectra are then drawn and com-



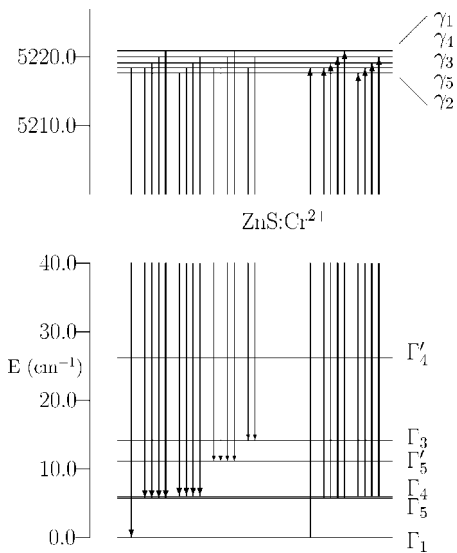


FIG. 5. Scheme of vibronic levels for ZnS:Cr<sup>2+</sup> leading to emissions (downward arrows) and absorptions (upward arrows). Clearly observed transitions are depicted by thick arrows, while thin arrows show the possible origin for some weak zero-phonon emission lines observed for the case of ZnS, but not to be observed for ZnSe due to background noise.

pared with experiment. This procedure is continued up to a point where energies and relative intensities of the lines resemble the experimental spectra as done above.

In Fig. 5 we present a diagram for the vibronic levels of both multiplets involved in the main transitions producing the observed emission (downward arrows) and absorption (upward arrows) spectra of ZnS:Cr<sup>2+</sup>.

**B. Results and discussion for ZnSe:Cr<sup>2+</sup>**

Similar to what was done for ZnS, an adjustment using  $\tau_2$  modes was also done for ZnSe, fixing the values of the parameters to obtain the desired separation of 7 cm<sup>-1</sup> in this case; they are  $\hbar\omega_\tau=70$  cm<sup>-1</sup> and  $E_{JT}^{(\tau)}=180$  cm<sup>-1</sup> and  $E'_{JT}=270$  cm<sup>-1</sup>. The calculated spectrum is shown in Fig. 6, presenting a threshold peak at 4971 cm<sup>-1</sup>, then a higher and wider band centered at 4964 cm<sup>-1</sup>, as measured in the experiment.<sup>10,11</sup> The lower and wider band expected around 4940 cm<sup>-1</sup> cannot be compared to the experiment in this case because of the presence of huge background noise due to phonon assisted transitions immediately under 4960 cm<sup>-1</sup>. For the values of the parameters already obtained from fitting the luminescence spectrum the absorption spectra is now evaluated directly at liquid helium temperature giving the spectrum presented in Fig. 7, which is in excellent agreement with the experimental curve. The very weak band before the main line (here at 4971 cm<sup>-1</sup>) is due to transitions starting from excited vibronic levels and the quenching produced by the Boltzmann population factor results here is more effective than in ZnS:Cr<sup>2+</sup>, where the energy splitting among excited and ground levels is smaller. It is also possible to draw an energy level diagram to illustrate absorptions and emissions. However, we omit it here since such diagram is similar to the one valid for ZnS:Cr<sup>2+</sup>

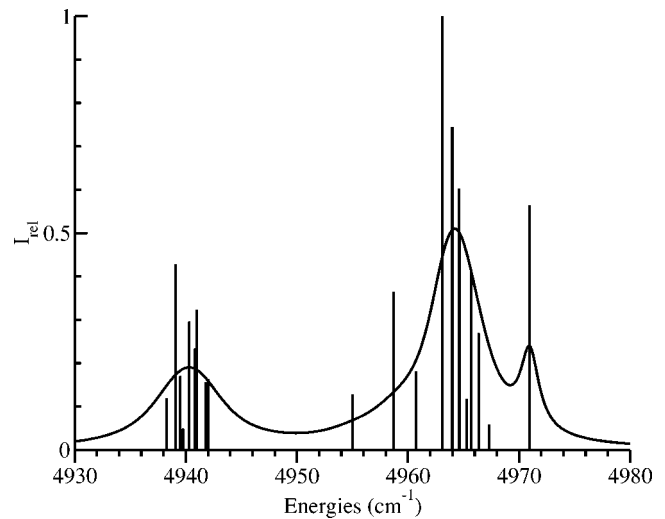


FIG. 6. Emission spectrum for ZnSe:Cr<sup>2+</sup> predicted by coupling <sup>5</sup>T<sub>2</sub> multiplets to  $\tau_2$  modes;  $\hbar\omega_\tau=70$  cm<sup>-1</sup>,  $E_{JT}^{(\tau)}=180$  cm<sup>-1</sup>, and  $E'_{JT}=270$  cm<sup>-1</sup>.

given in Fig. 5, after appropriate adjustments in the actual energy of the levels.

**C. General comments for both ZnS:Cr<sup>2+</sup> and ZnSe:Cr<sup>2+</sup>**

Perhaps the most striking feature of this analysis is that by trying to explain the optical spectra in either case, we found once again the same or very close coupling acoustic frequencies as previously reported for other *d<sup>n</sup>* magnetic impurities in the same compounds.

Thus, for instance, for the case of Fe<sup>2+</sup>, which is a <sup>5</sup>D system too, coupling frequencies were found to be 90 cm<sup>-1</sup> for ZnS and 70 cm<sup>-1</sup> for ZnSe.<sup>23</sup> For the case of V<sup>2+</sup>, another *d* system, coupling acoustic frequencies were once again 100 cm<sup>-1</sup> for ZnS and 70 cm<sup>-1</sup> for ZnSe.<sup>17</sup> It seems then that the *d* electronic cloud around the impurity is most sensitive to particular phonons of these frequencies in

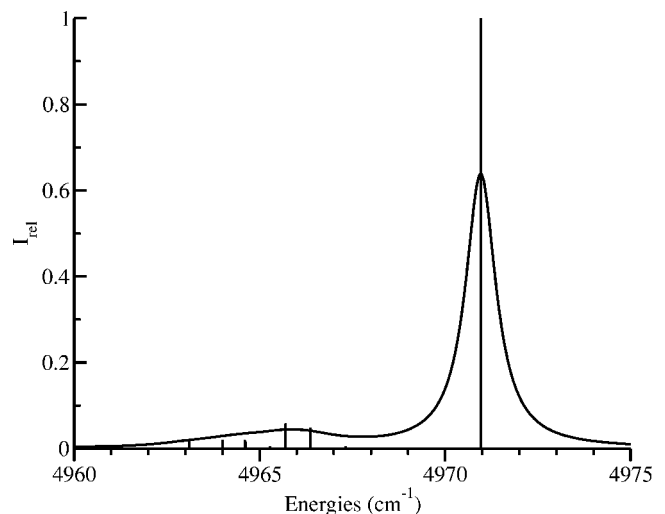


FIG. 7. Absorption spectrum for ZnSe:Cr<sup>2+</sup> directly calculated using the same wave functions used to calculate emission spectrum.

these compounds. By looking at the lattice dynamics of ZnS and ZnSe<sup>24-26</sup> it is found that such phonons are abundant and correspond to points  $TA_1(K)$  in the lattice dynamics of both compounds. Moreover, these points in the Brillouin zone have local components  $\epsilon$  and  $\tau_2$  precisely as required.<sup>27</sup>

It is now also understood why it is not possible to get a clear spectra for the cases ZnTe:Cr<sup>2+</sup> and CdTe:Cr<sup>2+</sup>. Lattice dynamics in these compounds<sup>24,28</sup> present very low acoustical frequencies producing a large mixing of many zero-phonon lines with phonon-assisted lines making it impossible to recognize individual lines. The result is the production of a broad band with a structure depending on the impurity concentration, and spectrometer resolution. Theoretically, it is possible to obtain appropriate shapes varying a large number of linewidths. However, this is not the approach followed in the present paper where we have concentrated on the clear zero-phonon lines present in ZnS:Cr<sup>2+</sup> and ZnSe:Cr<sup>2+</sup>, close to the broad band. Unfortunately, for ZnTe:Cr<sup>2+</sup> and CdTe:Cr<sup>2+</sup> such lines are absorbed within the broad band and the analysis performed here is not possible.

#### IV. CONCLUDING REMARKS

The main features associated to zero phonon lines in the absorption and emission spectra of Cr<sup>2+</sup> in both ZnS and ZnSe can be explained by introducing a vibronic coupling to the Hamiltonian. However,  $\epsilon$  modes do not account for intensities of the observed lines. Then,  $\tau_2$  modes were introduced giving a very good description of energy levels and intensities of the associated electric-dipole transitions in both compounds.

In the case of ZnS the coupling mode has energy 100 cm<sup>-1</sup>, which is very close to the coupling phonon energy of other similar ions in this same compound. The upper multiplet is compressed to a multiplet with a spread of about 3 cm<sup>-1</sup> by means of a JT energy of over 300 cm<sup>-1</sup>. The coupling to the lower multiplet gives good results for a JT energy of about 260 cm<sup>-1</sup>. This Huang-Rhys factor in this case is  $S_{\tau}=2.6$ , which corresponds to an intermediate JT coupling.

Similarly, for ZnSe the coupling mode has an energy corresponding to the same point of the Brillouin zone as the previous one ( $TA_1(K)$ ), namely, 70 cm<sup>-1</sup> in this case. The upper multiplet is again concentrated in a few cm<sup>-1</sup>. The coupling to the lower multiplet is of similar strength as in previous case. Namely, the best adjustment is reached for a JT energy close to 180 cm<sup>-1</sup>, leading to  $S_{\tau}\approx 2.6$ .

The rather high values of Huang-Rhys factors, particularly on the upper multiplet, as commented in previous paragraphs, are in good correspondence with previous estimates proposing even a possible static JT case for these systems.<sup>8-10</sup> Independent of the words used to describe the coupling, the effect is certainly to mix largely the pure electronic levels producing two bands of transitions in both absorption and emission instead of many zero-phonon lines observed for weaker coupling.

#### ACKNOWLEDGMENTS

The following agencies and programs are acknowledged for partial support: Fondecyt (Chile) under Contract No. 1020993; International Collaboration CNR (Italy) and Conicyt (Chile); Millennium Nucleus "Condensed Matter Physics" (Mideplan Chile P02-054-F); Dirección de Investigación y Desarrollo Universidad de La Frontera.

- 
- <sup>1</sup>J.T. Vallin, G.A. Slack, S. Roberts, and A.E. Hughes, *Phys. Rev. B* **2**, 4313 (1970).  
<sup>2</sup>H. Nelkowsky and G. Grebe, *J. Lumin.* **1/2**, 88 (1970).  
<sup>3</sup>G. Grebe and H.-J. Schulz, *Phys. Status Solidi B* **54**, K69 (1972); *Z. Naturforsch. A* **29A**, 1803 (1974).  
<sup>4</sup>J.T. Vallin and G.D. Watkins, *Phys. Rev. B* **9**, 2051 (1974).  
<sup>5</sup>G. Grebe, G. Roussos, and H.-J. Schulz, *J. Lumin.* **12/13**, 701 (1976); *J. Phys. C* **9**, 4511 (1976).  
<sup>6</sup>A.L. Natadze and A.I. Ryskin, *Solid State Commun.* **24**, 147 (1977).  
<sup>7</sup>M. Kaminska, J.M. Baranowski, S.M. Uba, and J.T. Vallin, *J. Phys. C* **12**, 2197 (1979).  
<sup>8</sup>D. Colignon, E. Kartheuser, S. Rodriguez, and M. Villeret, *J. Cryst. Growth* **159**, 875 (1996).  
<sup>9</sup>G. Goetz and H.-J. Schulz, *Solid State Commun.* **84**, 523 (1992).  
<sup>10</sup>G. Goetz, H. Zimmermann, and H.-J. Schulz, *Z. Phys. B: Condens. Matter* **91**, 429 (1993).  
<sup>11</sup>G. Goetz, Doctoral thesis, Technischen Universität Berlin, 1991.  
<sup>12</sup>A.S. Abhvani, C.A. Bates, B. Clerjaud, and D.R. Pooler, *J. Phys. C* **15**, 1345 (1982).  
<sup>13</sup>H. Katayama-Yoshida and K. Sato, *Physica B* **327**, 337 (2003).  
<sup>14</sup>E.E. Vogel, M.A. de Ore, J. Rivera-Iratchet, H.-J. Schulz, and M.U. Lehr, *Phys. Rev. B* **54**, 13 424 (1996).  
<sup>15</sup>I.B. Bersuker, *Electronic Structure and Properties of Transition Metals Compounds* (Wiley, New York, 1996).  
<sup>16</sup>I.B. Bersuker and V.Z. Polinger, *Vibronic Interactions in Molecules and Crystals* (Springer, Berlin, 1989).  
<sup>17</sup>G. Bevilacqua, L. Martinelli, and E.E. Vogel, *Phys. Rev. B* **66**, 155338 (2002).  
<sup>18</sup>M. D. Sturge, in *Solid State Physics*, edited by F. Seitz, D. Turnbull, and H. Ehrenreich (Academic, New York, 1967), Vol. 20.  
<sup>19</sup>C. Lanczos, *J. Res. Natl. Bur. Stand.* **45**, 255 (1950); **49**, 33 (1952); *Applied Analysis* (Prentice-Hall, Englewood Cliffs, NJ, 1956).  
<sup>20</sup>R. Haydock, V. Heine, and M. J. Kelly, *J. Phys. C* **5**, 2845 (1972); **8**, 2591 (1975); see also D. W. Bullen, R. Haydock, and M. J. Kelly, in *Solid State Physics*, edited by H. Ehrenreich, F. Seitz, and D. Turnbull (Academic, New York 1980), Vol. 35.  
<sup>21</sup>L. Martinelli, M. Passaro, and G. Pastori Parravicini, *Phys. Rev. B* **40**, 10 443 (1989).  
<sup>22</sup>L. Martinelli, G. Bevilacqua, J. Rivera-Iratchet, M.A. de Ore, O. Mualin, E.E. Vogel, and J. Cartes, *Phys. Rev. B* **62**, 10 873 (2000).  
<sup>23</sup>O. Mualin, E.E. Vogel, M.A. de Ore, L. Martinelli, G. Bevilac-

- qua, and H.-J. Schulz, Phys. Rev. B **65**, 035211 (2002).
- <sup>24</sup>N. Vagelatos, D. Wehe, and J. King, J. Chem. Phys. **60**, 3613 (1974).
- <sup>25</sup>B. Hennion, F. Moussa, G. Pepy, and K. Kunc, Phys. Lett. **36A**, 376 (1971).
- <sup>26</sup>H.-Matsuo Kagaya and T. Soma, Phys. Status Solidi B **124**, 37 (1984).
- <sup>27</sup>F.S. Ham and G.A. Slack, Phys. Rev. B **4**, 777 (1971).
- <sup>28</sup>J.M. Rowe, R.M. Nicklow, D.L. Price, and K. Zanio, Phys. Rev. B **10**, 671 (1974).